

# Compositional and crystallographic changes on enamel when irradiated by Nd:YAG or Er,Cr:YSGG lasers and its resistance to demineralization when associated with fluoride

ZeZell, D.M.<sup>1</sup>; Ana, P.A.<sup>1</sup>; Benetti, C.<sup>1</sup>; Goulart, V.P.<sup>1</sup>; Bachmann, L.<sup>2</sup>; Tabchoury, C.P.M.<sup>3</sup>; Cury, J.A.<sup>3</sup>

1 – Instituto de Pesquisas Energéticas e Nucleares, IPEN-CNEN/SP, São Paulo, SP, Brasil

2 – Faculdade de Filosofia, Ciências e Letras de Ribeirão Preto, USP, Ribeirão Preto, Brasil

3 – Faculdade de Odontologia de Piracicaba, UNICAMP, Piracicaba, SP, Brasil

## ABSTRACT

This study investigated the compositional and crystallographic changes on enamel when irradiated by Er,Cr:YSGG ( $\lambda=2.78\mu\text{m}$ ,  $8.5\text{J}/\text{cm}^2$ ) or Nd:YAG ( $\lambda=1064\text{nm}$ ,  $84.9\text{J}/\text{cm}^2$  associated with black coating), its resistance to demineralization when irradiation is associated with fluoride (APF-gel), and  $\text{CaF}_2$ -like material formation and retention. Sample surfaces were analyzed by ATR-FTIR ( $4000\text{--}650\text{cm}^{-1}$ ,  $4\text{cm}^{-1}$ ) resolution. Irradiation with Er,Cr:YSGG laser promoted a significant decrease on carbonate content of enamel. After Nd:YAG irradiation, it was observed a significant decrease of carbonate and amides I and II. X-ray diffraction showed that both laser irradiations promoted formation of  $\alpha$ -tricalcium phosphate and tetracalcium phosphate, and a significant increase on the crystal growth of the enamel apatite (ANOVA,  $p<0.05$  was used for all analysis). These changes can explain the improved resistance of enamel to demineralization observed in the second part of the study, in which 240 enamel slices were divided in 8 groups, received 4 min of professional fluoride gel (APF-gel 1.23%F) applied before or after irradiation. After treatments, the formation of calcium fluoride ( $\text{CaF}_2$ ) was determined. The remaining slabs of each group were submitted to a 10-day pH-cycling model and, subsequently, enamel demineralization was evaluated by cross-sectional microhardness. Both lasers significantly reduced enamel demineralization (ANOVA,  $p<0.05$ ), and the previous APF-gel application followed by laser showed the higher reduction of enamel demineralization.  $\text{CaF}_2$  formed before pH-cycling was significantly higher in groups where APF was associated with laser irradiation. After demineralization, these groups also presented higher  $\text{CaF}_2$  retention in respect to isolated treatments (only APF or only laser), suggesting its anticaries potential.

## KEYWORD LIST

Lasers  
Enamel  
Fluoride  
ATR-FTIR  
Crystallography  
X-ray diffraction  
Demineralization  
Caries Prevention

## 1. INTRODUCTION

The decline in dental caries over the last few decades has been attributed to the extensive use of fluoride. Although fluoride is the most powerful treatment to prevent tooth decay, the development of new methods to completely control this disease is still necessary, mainly in developing countries. In this way, lasers, combined or not with fluoride, have been tested on teeth to improve dental enamel properties in order to enhance its resistance to demineralization<sup>1,2,3,4,5</sup>.

The use of laser irradiation for preventing dental caries is based on the chemical and physical properties of the enamel due to the heating of the surface. Depending on the temperature reached, laser irradiation can promote loss of water and carbonate (between 100°C and 1100°C)<sup>6,7</sup>, oxidation of phosphates and formation of pyrophosphates (between 100°C and 650°C)<sup>8,9</sup>, and the formation of new crystalline phases ( $\alpha$ -TCP and  $\beta$ -TCP phases in temperatures up to 1100°C)<sup>10</sup>.

Nd:YAG lasers have been suggested as a potential tool for caries prevention<sup>1</sup> due to the heating effects on enamel surface, evidenced mainly by the melting and recrystallization process, with indicates temperature ranges up to 1200°C<sup>11</sup>. Although Nd:YAG laser is poorly absorbed by dental hard tissues, the application of a dark dye on enamel restricts laser absorption on the surface. On the other hand, Er,Cr:YSGG laser photons are highly absorbed by the hydroxyl ions of both water and hydroxyapatite<sup>2,12</sup>, and can increase the enamel temperature up to 212°C when used at 8.5 J/cm<sup>2</sup><sup>13</sup>. Considering these temperature findings, Nd:YAG and Er,Cr:YSGG can be considered promissory alternatives for preventing demineralization, which was previously suggested by some *in vitro*<sup>2,5</sup>, *in situ*<sup>3,4</sup> and clinical<sup>1</sup> studies reported on literature.

Laser irradiation, combined with topical fluoride treatment, can induce an even greater increase in caries resistance, which was previously reported for different laser wavelengths<sup>8,14,15</sup>. However, concerning the use of Nd:YAG and Er,Cr:YSGG lasers, the explanation of the chemical changes induced on dental enamel, and how laser can interact with fluoride leading to the increase of resistance of enamel to demineralization, is still not completely known. In this way, the purpose of this study was to investigate the chemical and crystallographic changes on dental enamel after irradiation with Nd:YAG and Er,Cr:YSGG at parameters aimed at caries prevention, and to evaluate the effect of these lasers, when associated with professional application of fluoride, on fluoride formation and retention, and also the potential of this association to prevent dental caries.

## 2. MATERIAL AND METHODS

### 2.1. Analysis of compositional and crystallographic changes on enamel

21 sound enamel slabs (4 x 4 x 2 mm) were obtained from smooth surfaces of 7 third human molar teeth (IPEN Ethics Committee approval # 094-2004), and were randomized in three treatment groups of 7 specimens each: G1 – untreated enamel surface; G2 – enamel irradiated with Er,Cr:YSGG laser; G3 – enamel irradiated with Nd:YAG laser. 5 samples of each experimental group were submitted for compositional analysis by ATR-FTIR, while 2 samples of each experimental group were submitted for crystallographic analysis by X-ray diffraction.

The Nd:YAG laser irradiation on enamel was performed using a Pulse Master 1000 laser (ADT - USA), at 1.064  $\mu\text{m}$ , with a 300  $\mu\text{m}$  quartz fiber optic delivery system and temporal width of 100  $\mu\text{s}$ . Before irradiations, all enamel surfaces were recovered with a coal paste<sup>11</sup>, and the irradiations were performed at 10 Hz repetition rate, 0.6 W, energy density of 84.9 J/cm<sup>2</sup> and 60 mJ per pulse<sup>1</sup>. Laser tip was kept in contact with the surfaces, after positioning in optical supports coupled to the computer controlled motion system with speed adjusted to 0.98 mm/s.

The Er,Cr:YSGG laser irradiation on enamel was performed using an Er,Cr:YSGG hydrokinetic laser device (Millenium, Biolase Inc., USA), at wavelength of 2.78  $\mu\text{m}$ , pulse width of 140  $\mu\text{s}$  and repetition rate of 20 Hz. In this study, samples were irradiated at 32.5 mJ/pulse, 0.75 W and 8.5 J/cm<sup>2</sup>, using a S75 tip (sapphire terminal of 750  $\mu\text{m}$  diameter and 6 mm long)<sup>5</sup>. During laser irradiation, laser handpiece was positioned in optical supports coupled to a computer controlled motion system (Newport, Irvine, CA), with speed adjusted to 4 mm/s<sup>13</sup>. Laser tip was kept at a standardized distance of 1 mm from enamel surface and laser irradiation scanned all area of enamel surface.

The compositional analysis was performed using the Attenuated Total Reflectance - Fourier transform infrared spectroscopy (ATR-FTIR - Thermo Nicolet Smart Orbit) with a DTGS detector using a diamond crystal, coupled to a FTIR spectrometer (6700 ThermoNicolet, USA). The ATR-FTIR spectra of each sample were obtained with 4.0 cm<sup>-1</sup> resolution, with 120 scans in the range of 4000 to 650 cm<sup>-1</sup>, and were recorded

using the OMNIC Spectra Software. Infrared bands considered for this study were 883 cm<sup>-1</sup> to 1070 cm<sup>-1</sup> for phosphates and 1300 cm<sup>-1</sup> to 1600 cm<sup>-1</sup> for carbonates and organic contents. The center band positions and bands widths were obtained and the areas under the considered bands were calculated and normalized by phosphate band (1300–900 cm<sup>-1</sup>)<sup>16</sup> for semi-quantitative comparison between control and irradiated groups. The statistical analysis was performed using the OriginPro 8 software, considered the hypothesis testing to paired sample t test at 5% significance level.

The crystalline structure of the samples was evaluated by X-ray diffraction at a Synchrotron XRD1 beamline (LNLS, Campinas, Brazil), using a monochromatic X-ray beam with wavelength of 0.0954 nm<sup>10</sup>. The X-ray beam was configured at a grazing angle to maximize the surface diffraction signal and better detecting the possible new crystallographic phase produced after the laser irradiation. A step scanning diffractometer ( $2\theta_{\text{step}}=0.01^\circ$ ) equipped with a scintillator photon counter was used to record the diffraction spectra. In order to reduce the effect of statistical errors, a single diffraction pattern was obtained as the sum of the two individual recorded patterns.

For the crystalline plans (002), (210) and (300), the changes in crystal sizes were estimated using the Scherrer's equation:

$$D = \frac{K\lambda}{\beta \cos \theta}$$

where D is the mean crystallite size in the direction of corresponding plan; K is the shape factor;  $\lambda$  is the X-ray wavelength,  $\beta$  is the line broadening at half the maximum intensity (FWHM) in radians and  $\theta$  is the Bragg angle.

## 2.2. Analysis of resistance to demineralization and fluoride formation and retention

240 sound enamel slabs (4 x 4 x 2 mm) were obtained from smooth surfaces of 120 third human molar teeth, and were randomized in eight treatment groups of 30 specimens each: G1 – untreated enamel surface; G2 – treated with acidulated phosphate fluoride gel 1.23% F (APF gel - NuproGel®, Dentsply Industries, RJ, Brazil), pH 3.63 to 3.9, for 4 min<sup>17</sup>; G3- irradiated with Nd:YAG laser; G4- pre-irradiated with Nd:YAG and subjected to APF-gel application; G5- application of APF-gel and post-irradiation with Nd:YAG laser; G6- irradiated with Er,Cr:YSGG laser; G7- pre-irradiated with Er,Cr:YSGG and subjected to APF-gel application; G8- application of APF-gel and post-irradiation with Er,Cr:YSGG laser.

Both laser irradiations were performed at the same conditions to the described at the first part of this study. After treatments, CaF<sub>2</sub>-like material formation was analyzed in 10 samples of each experimental group. For that, samples were protected with wax #7 and individually immersed in plastic tubes containing 0.5 mL of 1.0 M KOH to extract the CaF<sub>2</sub>-like material retained in enamel after the pH-cycling<sup>18</sup>. After 24 h, the extracts were neutralized with 0.5 mL of TISAB II containing 1.0 M HCl.

The remaining 20 samples of each experimental group were submitted to a 10-day pH-cycling model<sup>19</sup>. For that, all surfaces of specimens were protected with an acid-resistant varnish, except for a circular area<sup>17</sup> of 3.14 mm<sup>2</sup> of enamel. During pH-cycling, the slabs were kept individually in a demineralizing solution for 3 h (6.37 mL/mm<sup>2</sup>) and in a remineralizing solution for 20 h (3.18 mL/mm<sup>2</sup>) each day, at 37° C. The demineralizing solutions were composed by 2.0 mM calcium, 2.0 mM phosphate, 0.03 ppm F<sup>-</sup> in 75 mM acetate buffer, pH 4.3, and the remineralizing solutions were composed by 1.5 mM calcium, 0.9 mM phosphate, 150 mM of KCl, 0.05 ppm F<sup>-</sup> in 20 mM cacodylic buffer, pH 7.4.

After pH-cycling, 10 slabs of each experimental group were longitudinally sectioned through the center of the exposed enamel, embedded in acrylic resin and analyzed by a FMARS FM 7386 (Future Tech, Kawasaki, Japan) microhardness tester with a Knoop diamond with 25 g load for 5 s<sup>19</sup>. Three rows of 12 indentations each were made, one in the central region of the dental enamel exposed and the other two 100  $\mu\text{m}$  below and above this; the indentations were made at 10  $\mu\text{m}$  from the outer enamel surface up to 160  $\mu\text{m}$ . The mean values at all measuring points at each distance from the surface were then averaged and expressed as Knoop hardness number (kg/mm<sup>2</sup>). The area of hardness loss (Delta S) was calculated by numerical integration using trapezoidal rule.

Also after demineralization, the remaining 10 samples of each experimental group were further submitted to the analysis of  $\text{CaF}_2$ -like material retained, using the same methodology as described before. All fluoride measurements were performed using an ion-selective electrode (Orion 96-09, Orion Research, MA, USA) and an ion analyzer (Orion 720 A+, Orion Research, Boston, MA, USA). The concentration of  $\text{CaF}_2$ -like material was expressed in  $\mu\text{gF}/\text{cm}^2$ . All results were analyzed by ANOVA (two-factor with replication) followed by Tukey's test. The results of  $\text{CaF}_2$ -like material were transformed by  $\log_{10}$ . For all analyses, 5% was considered the limit of significance and the software SPSS 13.0 for windows (SPSS Inc., Chicago, IL) was used.

### 3. RESULTS

#### 3.1. Analysis of compositional and crystallographic changes on enamel

The position of bands analyzed in the present study by ATR-FTIR is shown in Figure 1. Figure 2 shows the spectra of three different sets of enamel samples: non-irradiated, irradiated with  $\text{Er,Cr:YSGG}$  and irradiated with the  $\text{Nd:YAG}$  laser. In order to present the spectra in the same graphic, the spectra were normalized by phosphate band intensity ( $1300\text{--}900\text{ cm}^{-1}$ )<sup>16</sup>.

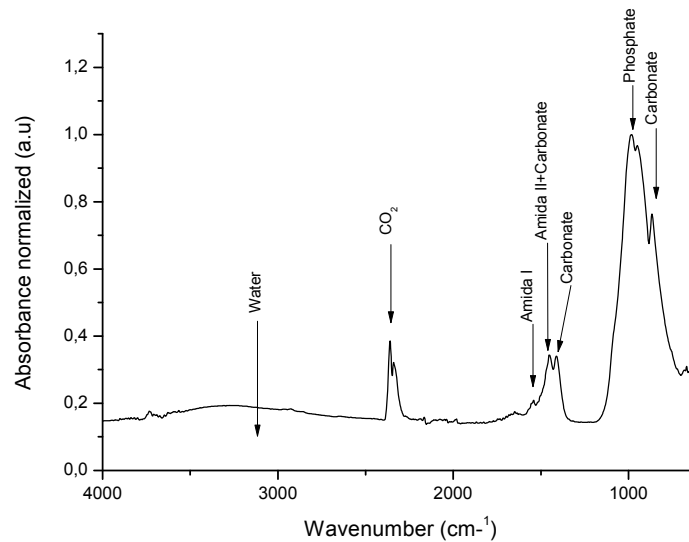


**Figure 1:** Infrared absorption spectrum of human dental enamel near  $400\text{--}4000\text{ cm}^{-1}$  with the identification of bands considered in this study.

The widths and center position peak of each considered band were measured before the normalization of the spectra, but no significant change was observed. Figure 3 evidences the differences in areas under the normalized bands between the same three sets of samples. It is possible to observe that the irradiation with both lasers significantly decreased the content of water, amides + carbonate, and carbonate contents.

The experimental X-ray diffraction patterns produced by enamel irradiated or not with  $\text{Er,Cr:YSGG}$  laser are both plotted in Figure 4. The position of Bragg peaks expected for hydroxyapatite (JCPDF 09-0432) are also indicated in the diffraction patterns. The database PDF2- Release (International Centre for Diffraction Data – ICDD, 2005) was used for indexing the additional peaks that were observed in the X-ray analysis. Our search did not directly lead to a known crystallographic phase for the observed set of additional Bragg peaks.

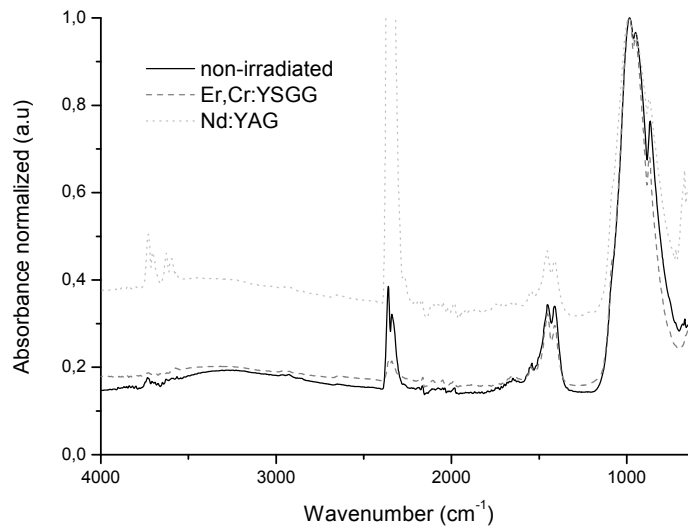


**Figure 2:** Infrared absorption spectra of enamel samples irradiated or not with Nd:YAG and Er,Cr:YSGG near 600–4000  $\text{cm}^{-1}$ .

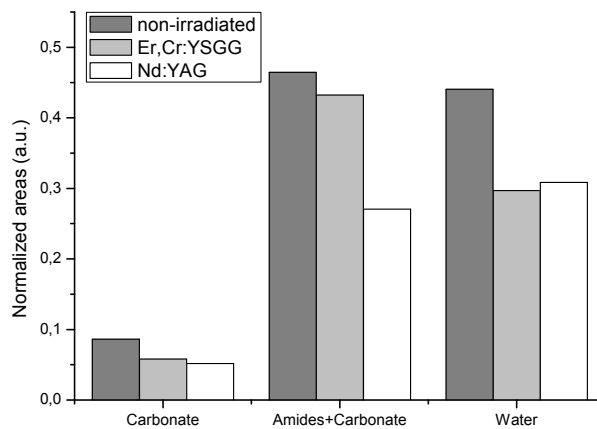


**Figure 3:** Average areas under the bands evidence the decrease of carbonate and water contents promoted by both lasers; however, only Nd:YAG promoted a significant decrease on organic content of enamel.

Observing the X-ray diffraction pattern corresponding to samples irradiated with Er,Cr:YSGG laser, it was evidenced a typical pattern of hydroxyapatite and other six additional peaks, corresponding to other crystalline phases. This finding indicates that the Er,Cr:YSGG (2.79  $\mu\text{m}$ ) laser irradiated enamel sample contains a mixture of at least two crystalline phases (Figure 4).

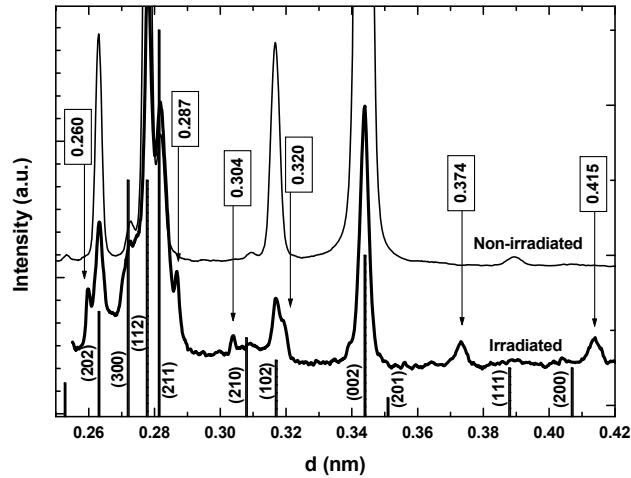


**Figure 4:** X-ray diffraction pattern of non-irradiated and irradiated human enamel with Er,Cr:YSGG laser. The main hydroxyapatite (HAP; JCPDF 09-0432) Bragg peaks and the identification of six new peaks, which are observed after irradiation.

To find the new phases, careful comparison was made with experimental diffraction pattern corresponding to irradiated enamel to  $\alpha$ -tricalcium phosphate ( $\alpha$ -TCP),  $\beta$ -tricalcium phosphate ( $\beta$ -TCP), and tetracalcium phosphate (TetCP) phases. These phases were previously observed after different types of laser irradiation or thermal treatments. Two of our experimental peaks (0.260 nm and 0.287 nm) match with  $\alpha$ -TCP phase. Considering the tricalcium phosphate in beta phase ( $\beta$ -TCP, JCPDF 09-0169), we observed in our study three diffraction peaks (0.260 nm, 0.287 nm, and 0.320 nm) that match to  $\beta$ -TCP peaks. For tetracalcium phosphate, most of the diffraction peaks of the expected pattern for TetCP match well to the Bragg peaks observed for irradiated enamel that are not present in the pattern produced by non-irradiated samples.

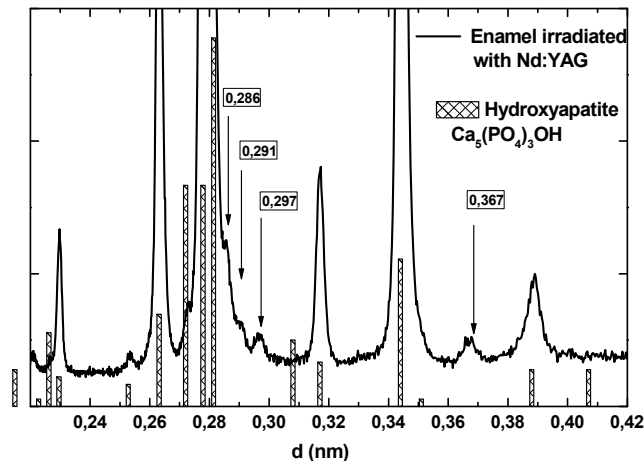


**Figure 5:** X-ray diffraction pattern of irradiated human enamel with Nd:YAG laser. The main hydroxyapatite (HAP; JCPDF 09-0432) Bragg peaks and the identification of four new peaks, which are observed after irradiation.

As to the cases of the samples irradiated with the Nd:YAG, the experimental X-ray diffraction patterns produced by the non-irradiated human enamel sample and another corresponding to enamel irradiated with laser are both plotted in Figure 5. The position of Bragg peaks expected for hydroxyapatite (JCPDF 09-0432) are, once again, also indicated in the diffraction patterns.

Like the Er,Cr:YSGG laser, the X-ray diffraction pattern corresponding to irradiated enamel displays a series of diffraction peaks similar to those observed for non-irradiated enamel. It also displays four additional peaks corresponding to a different crystallographic phase: 0.286 nm, 0.291 nm, 0.297 nm, and 0.367 nm.

The diffraction patterns of enamel irradiated with Nd:YAG were compared to the diffraction pattern of  $\alpha$ -tricalcium phosphate ( $\alpha$ -TCP),  $\beta$ -tricalcium phosphate ( $\beta$ -TCP), and tetracalcium phosphate (TetCP) and bruxite. These phases display peaks close to the ones observed after the Nd:YAG laser irradiation, although none of the structures displayed a perfect correlation with experimental values.

The estimation of changes of crystallite sizes on irradiated samples evidenced a decrease of the FWHM of crystalline plans (002) and (300) after enamel irradiation with Nd:YAG laser, and a decrease of the FWHM of crystalline plans (002) and (210) after enamel irradiation with Er,Cr:YSGG laser (Figure 6). There was no enough signal considering the plan (210) for Nd:YAG irradiated enamel. These results suggest an increase of crystallite sizes after laser irradiation.

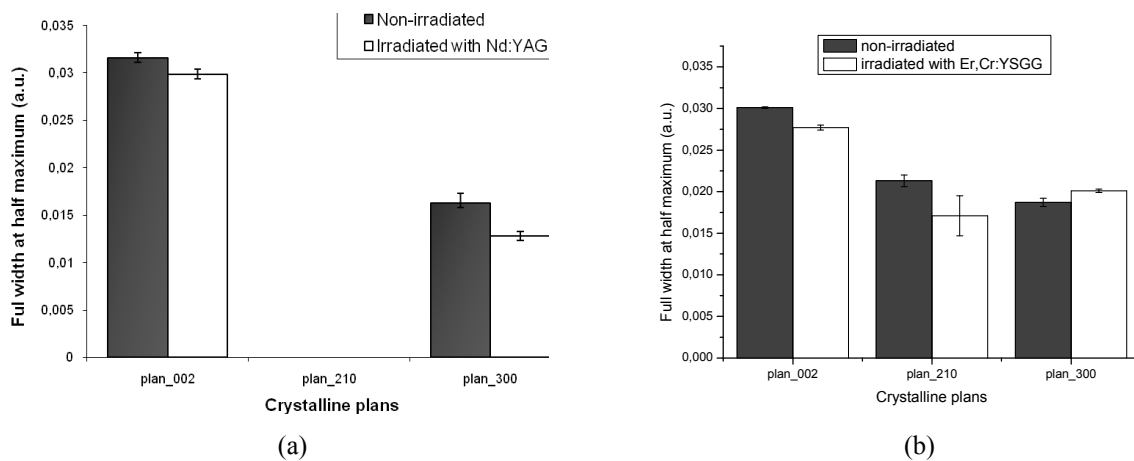


**Figure 6:** FWHM of crystalline plans (002), (210) and (300) of enamel irradiated with Nd:YAG (a) and Er,Cr:YSGG (b) when compared to non-irradiated enamel.

### 3.2. Analysis of resistance to demineralization and fluoride formation and retention

The isolated effect of the treatments showed (Table 1) that APF gel and both Nd:YAG and Er,Cr:YSGG lasers, at the parameters tested, were efficacious to reduce enamel demineralization in comparison with not treated control group ( $p < 0.05$ ). Also, although Nd:YAG and Er,Cr:YSGG laser combination with APF gel was more efficacious on reducing enamel demineralization when compared to the untreated group ( $p < 0.05$ ), no additive effect was found when these groups were compared with the APF group ( $p > 0.05$ ). These data are illustrated in Figure 6, showing that the caries lesion depth extended up to 100  $\mu\text{m}$  from the surface.

Regarding to  $\text{CaF}_2$ -like material formed and retained (Table 2), the results showed that although laser irradiation did not promote any increase ( $p > 0.05$ ) on  $\text{CaF}_2$ -like material formation ( $\text{CaF}_2$ -like material found immediately after irradiation) and retention ( $\text{CaF}_2$ -like material found after pH-cycling). When combined with APF gel application, although Er,Cr:YSGG laser irradiation promoted an augment of  $\text{CaF}_2$ -like material formation when compared to APF group, only enamel irradiation with Nd:YAG + APF caused a significant increase on  $\text{CaF}_2$ -like material formation ( $p < 0.05$ ). Also, it is possible to observe that there is a significant increase on fluoride retention after pH-cycling ( $p < 0.05$ ) on all irradiated samples when compared to APF group. Although in samples irradiated with Nd:YAG the fluoride retention is more evident in comparison with samples irradiated with Er,Cr:YSGG, this difference was not evidenced statistically.

**Table 1:** Means ( $\pm$  SD; n=10) of area of enamel hardness loss ( $\Delta S$ ) according to the treatments.

<i>Treatments</i>	<i><math>\Delta S</math> (<math>kg/mm^2 \times \mu m</math>)</i>
Untreated	$11899.3 \pm 2697.3^a$
APF	$7060.5 \pm 2806.8^b$
Nd:YAG	$6297.0 \pm 2796.9^b$
Nd:YAG + APF	$4490.5 \pm 2099.1^b$
APF + Nd:YAG	$4113.9 \pm 1406.9^b$
Er,Cr:YSGG	$7226.8 \pm 3838.6^b$
Er,Cr:YSGG + APF	$4275.4 \pm 2544.2^b$
APF + Er,Cr:YSGG	$5172.5 \pm 2313.6^b$

Distinct letters indicate statistical difference by the Tukey test ( $p < 0.05$ ).

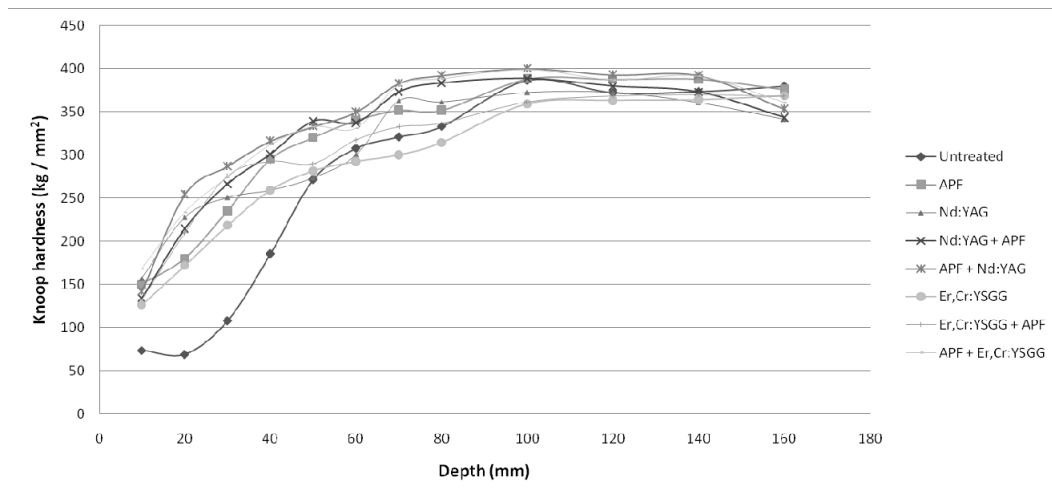


**Figure 6:** Means of enamel Knoop hardness ( $kg/mm^2$ ) according to treatments and the distance ( $\mu m$ ) from the surface.

**Table 2:** Means ( $\pm$  SD; n=10) of CaF<sub>2</sub> - like material (CaF<sub>2</sub>) concentration found on enamel before (formed) and after pH-cycling (retained), according to the treatments.

Treatment groups	CaF <sub>2</sub> ( $\mu\text{g F}^-/\text{cm}^2$ )	
	Formed	Retained
Untreated	2.46 $\pm$ 1.0 <sup>a</sup>	0.63 $\pm$ 0.2 <sup>d</sup>
APF	115.77 $\pm$ 38.8 <sup>b</sup>	24.39 $\pm$ 17.6 <sup>c</sup>
Nd:YAG	3.81 $\pm$ 0.9 <sup>a</sup>	2.21 $\pm$ 1.3 <sup>d</sup>
Nd:YAG + APF	448.20 $\pm$ 158.2 <sup>c</sup>	101.35 $\pm$ 49.4 <sup>b</sup>
APF + Nd:YAG	330.37 $\pm$ 142.6 <sup>b,c</sup>	58.61 $\pm$ 46.9 <sup>b</sup>
Er,Cr:YSGG	2.58 $\pm$ 0.5 <sup>a</sup>	1.90 $\pm$ 1.4 <sup>d</sup>
Er,Cr:YSGG + APF	216.31 $\pm$ 51.7 <sup>b</sup>	50.03 $\pm$ 22.8 <sup>b</sup>
APF + Er,Cr:YSGG	100.19 $\pm$ 45.0 <sup>b</sup>	59.14 $\pm$ 27.6 <sup>b</sup>

Distinct letters indicate statistical difference by the Tukey test ( $p < 0.05$ ).

#### 4. DISCUSSION

Although the use of infrared lasers for caries prevention is well documented in literature<sup>1,2,3,4,5,8,14,15</sup>, it is still necessary to know the exact mechanism of laser interaction with dental hard tissue and with fluoride in order to improve laser parameters and applications in dentistry. In this work, Nd:YAG and Er,Cr:YSGG lasers were evaluated considering that there is no study that investigates the chemical and crystallographic changes promoted by laser irradiated at parameters for caries prevention and their chemical interaction with fluoride.

In our study, it was possible to observe a decrease of water, carbonate and organic contents after both laser irradiations, with higher effects promoted by Nd:YAG laser. Considering that these chemical changes depend on temperature rises<sup>6,7</sup>, our findings confirm the evidence that Nd:YAG irradiation promotes higher surface temperatures when compared to the Er,Cr:YSGG laser when used at the energy densities of this work<sup>2,11,13</sup>. In previous studies, using Er,Cr:YSGG laser irradiation at similar parameters of this work, promotes temperature increments of approximately 212<sup>o</sup> C<sup>13</sup> and 400<sup>o</sup> C<sup>2</sup>, temperature range above the threshold for initial loss of water<sup>6,7</sup>, carbonates and proteins<sup>8,9</sup>. For this reason, even with less effects on enamel composition when compared to Nd:YAG laser irradiation, this study observed a slight chemical effects promoted by Er,Cr:YSGG laser, which confirms its potential for caries prevention.

An ATR-FTIR spectra band area corresponds to the amount of the corresponding component. For a quantitative comparison, it is necessary to normalize the spectra with a specific band area. Then, the normalization was made using the phosphate area band, once this is the more stable component of the enamel when thermal increase occurs<sup>7,20</sup>. The Amides + Carbonate band is specifically considered because both components have the same vibrational states, which makes it impossible to analyze them separately<sup>21</sup>.

It is important to notice that, during laser irradiation, the tissue temperature is not homogenous, but it depends on the depth and the zone of analysis. In this way, the characterization using the ATR-FTIR technique provides an average of the region analyzed, since it is not possible to differentiate regions that have suffered different temperature increments. In both non-irradiated and irradiated enamel spectra it was possible to verify all the analyzed components (water, amide, carbonate and phosphate). The material quantity analysis (Figure 3) suggests that both Er,Cr:YSGG and Nd:YAG laser irradiations tend to promote a decrease in the material content in the enamel. This phenomenon was observed in all the analyzed bands, but Nd:YAG irradiated samples showed a more intense decrease in the amide + carbonate content than the Er,Cr:YSGG irradiated samples. In both water and carbonate bands the difference is not so evident. The decrease in water, amides+carbonate and carbonate quantities probably occurs due to the increase in temperature in the samples during irradiation<sup>11</sup>. Given that the Er,Cr:YSGG laser is more absorbed by enamel than the Nd:YAG laser<sup>12</sup>,

temperature increases less in this case. For this reason, the decrease in organic components (amides + carbonate) is smaller than the observed for the Nd:YAG. However, further studies and higher samples number are necessary in order to confirm these findings.

Our X-ray diffraction study shows that irradiation with Er,Cr:YSGG and Nd:YAG of human dental enamel maintains a major phase corresponding to the hydroxyapatite  $[\text{Ca}_5(\text{PO}_4)_3\text{OH}]$  phase; however, it was also observed the formation of one or more minor crystalline phases. We have concluded that, within the angular domain analyzed, the additional crystalline phases produce six diffraction peaks corresponding to  $d$ -spacing ranging from 0.25 nm to 0.42 nm for Er,Cr:YSGG laser and four diffraction peaks corresponding to  $d$ -spacing ranging from 0.22 to 0.42 for Nd:YAG.

Concerning the Er,Cr:YSGG irradiated enamel, our observed experimental peaks match with some of the diffraction peaks corresponding to alpha and beta phases of tricalcium phosphate. The presence of several unmatched peaks led us to disregard the possibility for the new phase formed after irradiation to be ( $\alpha$ - or  $\beta$ -) TCP. However, we observed the formation of a single additional phase after Er,Cr:YSGG laser irradiation, which is probably tetracalcium phosphate (TetCP)<sup>22</sup>.

This result differs from what we have found after the Nd:YAG laser irradiation, which leads to TCP- $\alpha$  e TCP- $\beta$  formations. The difference concerning the crystalline phase observed after the Er,Cr:YSGG and the Nd:YAG laser irradiation owes mainly to the resulting high temperature generated during the irradiation<sup>2,11,13</sup>. This happens because the Nd:YAG laser presents lower absorption than the Er,Cr:YSGG laser<sup>12</sup>. The results obtained in this study agree with previous reports of literature concerning the formation of these phases on enamel irradiated with  $\text{CO}_2$  and Ho:YLF lasers<sup>10,23</sup>. The irradiation of enamel with these infrared lasers, similar than Nd:YAG, also promote melting and recrystallization of enamel, that indicates temperature increments up to 1200° C. These reported new crystalline phases are formed at high temperatures, up to 800° C for  $\beta$ -TCP<sup>24</sup> and up to 1100° C for  $\alpha$ -TCP and TetCP phases<sup>7</sup>, temperatures that justify the less crystalline changes on Er,Cr:YSGG irradiated enamel when compared to Nd:YAG laser irradiation.

In this study, we can observe an indicative signal of increment of crystallites size of hydroxyapatite after both laser irradiation, although the X-ray signal for crystalline plan (210) of Nd:YAG samples was not sufficiently strong for the measurement of FWHM. These changes probably are related to the temperature increase promoted by laser irradiation, as it was suggested previously in literature with heated hydroxyapatite<sup>25</sup>. This behavior was also observed on Nd:YAG irradiated dentin<sup>26</sup>, where it was demonstrated that the crystallite size increases according laser energy density.

After the simulation *in vitro* of a cariogenic challenge, the results of the present study (Table 1 and Figure 6) show that both laser irradiations were able to reduce the enamel loss of microhardness when compared to untreated group, which confirms that the chemical and crystalline changes promoted by laser irradiation can be the main responsible for reducing enamel demineralization. When associated with topical application of fluoride, independently of the order of treatments, it was shown a significant decrease on enamel loss of hardness when compared untreated group, which also corroborate with the reported in previous *in vitro*<sup>2,5,8</sup>, *in situ*<sup>3,4</sup> and *in vivo*<sup>1</sup> studies, demonstrating the efficiency of infrared lasers associated with fluoride on reducing enamel solubility even after follow-up of 1 year. Although it was not evidenced significant difference of laser and fluoride groups when compared to APF group, it was evidenced a reduction of 41.7% and 39.5% of loss of hardness in APF+Nd:YAG and Er,Cr:YSGG+APF groups, respectively, when compared to APF group, suggesting a synergism of laser and fluoride. This results agree with literature, mainly with the use of  $\text{CO}_2$  and Nd:YAG lasers, when laser irradiation after or before APF application reduced the initial enamel demineralization<sup>8,15</sup>, inhibited subsequent lesion progression<sup>14</sup> and enhanced fluoride adsorption<sup>27</sup> and retention<sup>28</sup>.

Together with the chemical and crystalline changes promoted by laser irradiation on enamel, the observed results of reducing enamel demineralization can be also explained by the significant increment of  $\text{CaF}_2$ -like material formation and retention observed in the present study in irradiated samples (Table 2). There are some theories suggested by literature to explain how laser interacts with fluoride, including the formation of “microspaces” in enamel that would facilitate the fluoride incorporation<sup>29</sup>; the induction of fluorapatite formation<sup>30</sup>, the increment of the diffusion of fluoride ions through the pores between the enamel rods<sup>15</sup> and the formation of fluoride reservoirs<sup>28</sup>. However, in the present study, it seems that the increment of  $\text{CaF}_2$ -like material formation and retention is a result of the morphological changes promoted by laser irradiation, considering the melting promoted by Nd:YAG<sup>11</sup> and slight ablation promoted by Er,Cr:YSGG<sup>13</sup>. In this way, the ablation sites could expose a higher number of hydroxyapatite crystals, which reacted with APF and, as a

consequence, a significant higher quantity of calcium fluoride was produced, which is in agreement with the theory that lased enamel could be more reactive to fluoride<sup>31</sup>.

Considering the results of the present study, it seems that the chemical modifications on dental enamel, such as the loss of carbonate and organic contents, the formation of new crystalline phases and the increment of crystallite sizes of hydroxyapatite, promoted by laser irradiation are the main mechanism to improve the resistance of this tissue to demineralization. Also, the synergism with fluoride is demonstrated, which can maintain the cariostatic effect for a longer period of time. However, clinical studies are necessary to corroborate this statement.

## 5. CONCLUSION

In conclusion, according to the conditions of the present study, Nd:YAG and Er,Cr:YSGG lasers lead the formation of new crystallographic phases on enamel and changed its composition, reducing carbonates, water and organic contents. The induced changes on enamel could be responsible for the effects of increasing the formation and retention of CaF<sub>2</sub>-like material observed, that can justify the effects on reducing enamel demineralization observed.

## 6. ACKNOWLEDGEMENTS

The authors would like to thank to FAPESP (Proc. 2006/06746-0), CEPOF-FAPESP (Proc. 05/51689-2), PROCAD-CAPES (Proc. 0349/05-4), INFO-CNPq (Proc. 573916/2008-0), Universal-CNPq (Proc. 473723/2007-7) and Laboratorio Nacional de Luz Sincrotron for government financial support for this investigation.

## REFERENCES

- [1] Zezell, D.M., Boari, H.G.D., Ana, P.A., Eduardo, C.P., Powel, G.L., "Nd:YAG laser in caries prevention: a clinical trial", *Lasers Surg. Med.* 41, 31-35 (2009).
- [2] Fried, D., Featherstone, J.D.B., Visuri, S.R., Seka, W.W., Walsh, J.T., "The caries inhibition potential of Er:YAG and Er,Cr:YSGG laser irradiation", *Proc. SPIE* 2672, 73-77 (1996).
- [3] Apel, C., Birker, L., Meister, J., Weiss, C., Gutknecht, N., "The caries preventive potential of subablative Er:YAG and Er:YSGG laser radiation in an intraoral model: a pilot study", *Photomed. Laser Surg.* 22, 312-317 (2004).
- [4] Korytnicki, D., Mayer, M.P., Daronch, M., Singer, J.M., Grande, R.H., "Effects of Nd:YAG laser on enamel microhardness and dental plaque composition: an in situ study", *Photomed. Laser Surg.* 24, 59-63 (2006).
- [5] Ana, P.A., Tabchoury, C.P.M., Cury, J.A., Zezell, D.M., "Effect of Er,Cr:YSGG laser and fluoride application on enamel demineralization", *Caries Res.* 41, 325-326 (2007).
- [6] Kuroda, S., Fowler, B.O., "Compositional, structural, and phase changes in in vitro laser-irradiated human tooth enamel", *Calcif. Tissue Int.* 36, 361-369 (1984).
- [7] Fowler, B.O., Kuroda, S., "Changes in heated and in laser-irradiated human tooth enamel and their probable effects on solubility", *Calcif. Tissue Int.* 38, 197-208 (1986).
- [8] Hsu, C.Y.S., Jordan, T.H., Dederich, D.N., Wefel, J.S., "Effects of low-energy CO<sub>2</sub> laser irradiation and the organic matrix on inhibition of enamel demineralization", *J. Dent. Res.* 79(9), 1725-1730 (2000).
- [9] Kantola, S., Laine, E., Tarna, T., "Laser-induced effects on tooth structure. X-ray diffraction study of dental enamel exposed to a CO<sub>2</sub> laser", *Acta Odontol. Scand.* 31(6), 369 - 379 (1973).
- [10] Bachmann, L., Craievich, A.F., Zezell, D.M., "Crystalline structure of dental enamel after Ho:YLF laser irradiation", *Arch. Oral. Biol.* 49, 923-929 (2004).
- [11] Boari, H.G.D., Ana, P.A., Eduardo, C.P., Powell, G.L., Zezell, D.M., "Absorption and thermal study of dental enamel when irradiated with Nd:YAG laser with the aim of caries prevention", *Laser Phys.* 19(7), 1463-1469 (2009).
- [12] Seka, W., Featherstone, J.D.B., Fried, D., Visuri S.R., Walsh J.T., "Laser ablation of dental hard tissue: from explosive ablation to plasma-mediated ablation", *Proc. SPIE* 2672, 144-158 (1996).

- 
- [13] Ana, P.A., Blay, A., Miyakawa, W., Zzell, D.M., "Thermal analysis of teeth irradiated with Er,Cr:YSGG at low fluences", *Laser Phys Letters*. 4, 827-830 (2007).
- [14] Santos, M.N., Fried, D., Hilo, M.R., Featherstone J.D.B., "Effect of a new carbon dioxide laser and fluoride on occlusal caries progression in dental enamel", *Proc. SPIE* 4610, 132-138 (2002).
- [15] Phan, N.D., Fried, D., Featherstone, J.D.B., "Laser-induced transformation of carbonated apatite to fluorapatite on bovine enamel", *Proc. SPIE* 3593, 233-239 (1999).
- [16] Heigl, J.J., Bell, M.F., White, J.U., "Application of infrared spectroscopy to the analysis of liquid hydrocarbons", *Anal. Chem.* 19, 293-298 (1947).
- [17] Delbem, A.C., Cury, J.A., "Effect of application time of APF and NaF gels on microhardness and fluoride uptake of in vitro enamel caries", *Am. J. Dent.* 15, 169-172 (2002).
- [18] Caslavská, V., Moreno, E.C., Brudevold, F., "Determination of the calcium fluoride formed from in vitro exposure of human enamel to fluoride solutions", *Arch. Oral Biol.* 20, 333-339 (1975).
- [19] Argenta, R.M.O., Tabchoury, C.P.M., Cury, J.A., "A modified pH-cycling model to evaluate fluoride effect on enamel demineralization", *Pesq. Odontol. Bras.* 17, 241-246 (2003).
- [20] Featherstone, J.D.B., Nelson, D.G.A., "Laser effects on dental hard tissue", *Adv. Dent. Res.* 1, 21-26 (1987).
- [21] Sasaki, K.M., Aoki, A., Ichinose, S., Yoshino, T., Yamada, S., Ishikawa I., "Scanning Electron Microscopy and Fourier Transformed Infrared Spectroscopy Analysis of Bone Removal Using Er:YAG and CO<sub>2</sub> Lasers", *J. Periodontol.* 73(6), 643-651 (2002).
- [22] Bachmann, L., Rosa, K., Ana, P.A., Zzell, D.M., Craievich, A.F., Kellermann, G., "Crystalline structure of human enamel irradiated with Er,Cr:YSGG laser", *Laser. Phys. Lett.* 6(2), 159-162 (2009).
- [23] Nelson, D.G., Wefel, J.S., Jongbloed, W.L., Featherstone, J.D., "Morphology, histology and crystallography of human dental enamel treated with pulsed low-energy infrared laser radiation", *Caries Res.* 21, 411-426 (1987).
- [24] Sakae, T., "X-ray diffraction and thermal studies of crystals from the outer and inner layers of human dental enamel", *Arch. Oral Biol.* 33, 707-713 (1988).
- [25] Haberki, K., Bucko, M.M., Brzezinska-Miecznik, J., Haberko, M., Mozgawa, M.W., Panz, T., Pyda, A., Zarebski, J., "Natural hydroxyapatite – its behavior during heat treatment", *J. Eur. Ceramic. Soc.* 26, 537-542 (2006)
- [26] Arianto, Y.K.E., Bo, N.P., Akbar, S.M.S., "The effect of Nd : YAG laser irradiation on the microstructure of human dentin", 2nd International Conference on Advanced Materials Processing - ADVANCED MATERIALS PROCESSING II Book Series: MATERIALS SCIENCE FORUM. 437(4), 281-284 (2003).
- [27] Tagomori, S., Morioka, T., "Combined effects of laser and fluoride on acid resistance of human dental enamel", *Caries Res* 54: 15-7 (1989).
- [28] Nammour, S., Demortier, G., Florio, P., Delhaye, Y., Pireaux, J.J., Morciaux, Y., Powell, L., "Increase of enamel fluoride retention by low fluence argon laser in vivo", *Lasers Surg. Med.* 33, 260-263 (2003).
- [29] Oho, T., Morioka, T., "A possible mechanism of acquired acid resistance of human dental enamel by laser irradiation", *Caries. Res.* 24, 86-92 (1990).
- [30] Meurman, J.H., Hemmerle, J., Voegel, J.C., Rauhamaa-Makinen, R., Luomanen, M., "Transformation of hydroxyapatite to fluorapatite with high-energy CO<sub>2</sub> laser", *Caries Res.* 31, 397-400 (1997).
- [31] Hossain, M.M., Hossain, M., Kimura, Y., Kinoshita, J., Yamada, Y., Matsumoto, K. "Acquired acid resistance of enamel and dentin by CO<sub>2</sub> laser irradiation with sodium fluoride solution", *J. Clin. Laser Med. Surg.* 20, 77-82 (1997).